Tankyrase-2 oligomerizes with tankyrase-1 and binds to both TRF1 (telomere-repeat-binding factor 1) and IRAP (insulin-responsive aminopeptidase)

Juan I. SBODIO*, Harvey F. LODISH†‡ and Nai-Wen CHI*[1]

*Department of Medicine, University of California, San Diego, La Jolla, CA 92093-0673, U.S.A., †Whitehead Institute for Biomedical Research, 9 Cambridge Center, Cambridge, MA 02142, U.S.A., and ‡Department of Biology, Massachusetts Institute of Technology, Cambridge, MA 02142, U.S.A.

The poly(ADP-ribose) polymerase (PARP) tankyrase-1 contains an ankyrin-repeat domain that binds to various partners, including the telomeric protein TRF1 (telomere-repeat-binding factor 1) and the vesicular protein IRAP (insulin-responsive aminopeptidase). TRF1 binding recruits tankyrase-1 to telomeres and allows its PARP activity to regulate telomere homoeostasis. By contrast, IRAP binding and the Golgi co-localization of tankyrase-1 with IRAP might allow tankyrase-1 to affect the targeting of IRAP-containing vesicles. A closely related protein, tankyrase-2, has also been implicated in vesicular targeting. Unlike tankyrase-1, tankyrase-2 has not been shown to have PARP activity. In addition, it has not been implicated in telomere homoeostasis, because it did not interact with TRF1 in previous studies. Here we show that tankyrase-2 contains intrinsic PARP activity and, like tankryase-1, binds to both TRF1 and IRAP. Our analysis suggests that the ankyrin (ANK) domain of tankyrase-2 comprises five subdomains that provide redundant binding sites for IRAP. Moreover, tankyrase-2 associates and co-localizes with tankyrase-1, suggesting that both tankyrases might function as a complex. Taken together, our findings indicate that tankyrase-1 and tankyrase-2 interact with the same set of proteins and probably mediate overlapping functions, both at telomeres and in vesicular compartments.

Key words: ankyrin, poly(ADP-ribosyl)ation, telomeres, vesicles.

INTRODUCTION

Tankyrase-1 is a modular protein that consists of distinct domains [1]. The N-terminal HPS domain contains multiple runs of histidine, proline and serine residue homopolymers. The ankyrin (ANK) domain near the N-terminus comprises 24 consecutive ANK repeats that interact with various partners. This domain is followed by another protein interaction motif called the sterile α module (SAM) [2]. The C-terminal region of tankyrase-1 contains a poly(ADP-ribose) polymerase (PARP) domain. This domain can use NAD^+ as a cofactor *in vitro* to poly(ADP-ribosyl)ate tankyrase-1 itself and also the interacting partners of its ANK domain [1,3].

Tankyrase-1 is expressed in many tissues and targeted to various intracellular compartments [1,3,4]. It was identified first in HeLa cell nuclei as a telomeric PARP [1]. Although lacking an NLS (nuclear localization signal), tankyrase-1 is recruited to human telomeres through binding of its ANK domain to the telomeric protein TRF1 (telomere-repeat-binding factor 1) [4]. TRF1 acts to shorten the length of telomeres [5]. Interestingly, tankyrase-1 can poly(ADP-ribosyl)ate TRF1 *in vitro* and attenuate its affinity for telomeric DNA [1]. Indeed, when tankyrase-1 is tagged with an NLS and overexpressed in the nucleus, the immunostaining of TRF1 at telomeres is lost [6]. More importantly, the intranuclear overexpression of tankyrase-1, but not that of a PARP-deficient derivative, causes the lengthening of telomeres [6]. Tankyrase-1 was therefore proposed to offset the negative effect of TRF1 on telomere length [6].

Despite the effect of tankyrase-1 on telomeres, most tankyrase-1 protein is found in the cytoplasm in the vicinity of centrosomes. It is targeted to the pericentriolar domain of centrosomes during mitosis [4]. When the Golgi apparatus coalesces after mitosis toward centrosomes [7], tankyrase-1 associates with the Golgi as a peripheral membrane protein [3]. Golgi-associated tankyrase-1 has been speculated to regulate the targeting of 'GLUT4 vesicles' [3]. Found primarily in adipocytes and myocytes, these vesicles contain two important transmembrane proteins: the glucose transporter GLUT4 and IRAP (insulin-responsive aminopeptidase) [8–10]. GLUT4 vesicles are remarkable for their insulin-regulated targeting [8]. In the absence of stimulation by insulin, they reside in the Golgi and throughout the cytoplasm. On stimulation by insulin, GLUT4 vesicles undergo exocytosis to deposit their cargo in the plasma membrane. The exocytosis of these vesicles thus mediates two important insulin effects: the uptake of glucose through GLUT4 and the degradation of various vasoactive hormones by IRAP [11,12]. The acute insulin effect on GLUT4 translocation is mediated through the activation of phosphoinositide 3-kinase [12]. However, constitutive activation of the mitogen-activated protein (MAP) kinase cascade also increases the amount of cellular GLUT4 that is targeted to the cell surface ([13,14], but see also [15,16]). It is not yet known how GLUT4 vesicles are engaged by signalling molecules in either the phosphoinositide 3-kinase or the MAP kinase cascade.

In a search for signalling molecules that contact GLUT4 vesicles, we found that GLUT4 vesicles in the Golgi co-localize with tankyrase-1 [3]. The co-localization presumably reflects a direct interaction, because tankyrase-1 binds directly to a hexapeptide (R^{96}QSPDG^{101}; single-letter amino acid codes) in the IRAP cytosolic domain (residues 1–109) [3]. Interestingly, tankyrase-1 is a signalling molecule in the MAP kinase cascade.

Abbreviations used: ANK domain, ankyrin domain; GST, glutathione S-transferase; HA, haemagglutinin; HPS, histidine, proline and serine; IRAP, insulin-responsive aminopeptidase; MAP kinase, mitogen-activated protein kinase; NLS, nuclear localization signal; PARP, poly(ADP-ribose) polymerase; SAM, sterile α module; TRF1, telomere-repeat-binding factor 1.

[1] To whom correspondence should be addressed (e-mail nwchi@ucsd.edu).

On stimulation by insulin or growth factor, tankyrase-1 becomes stoichiometrically phosphorylated by MAP kinases; this *in vivo* phosphorylation enhances the PARP activity of tankyrase-1 *in vitro* [3]. We therefore proposed tankyrase-1 as a MAP kinase effector whose PARP activity regulates the targeting of GLUT4 vesicles [3].

Tankyrase-1 protein shares 83% sequence identity with a homologue that lacks the HPS domain but contains an otherwise identical domain structure [17]. This protein, tankyrase-2, was first known as a tumour antigen that elicits autoantibodies in certain tumour patients [18,19]. Subsequently, the ANK domain of tankyrase-2 was shown to bind to Grb14, a member of the SH2-containing family of adapters founded by Grb7 [17]. Like tankyrase-1, tankyrase-2 associates with the vesicular compartments: it co-purifies with a Golgi marker in the low-density microsomal fraction and it immunostains in a punctate cytosolic pattern [17]. Tankyrase-2 was therefore proposed, by analogy with tankyrase-1, as a link between signalling events and vesicular targeting [17]. Despite its extensive homology with tankyrase-1, tankyrase-2 has yet to be authenticated as a PARP. Moreover, tankyrase-2 reportedly differs from tankyrase-1 in that its ANK domain did not interact with TRF1 in a yeast two-hybrid assay [17]. Tankyrase-2 has therefore not been implicated in telomere homoeostasis [17].

This study characterizes tankyrase-2 and compares it with tankyrase-1. We confirmed that tankyrase-2 has intrinsic PARP activity and that this activity depends on the Met^{1054} residue in its PARP domain. We also showed that tankyrase-2, like tankyrase-1, binds to IRAP *in vivo* and *in vitro*. Unexpectedly, we found that tankyrase-2 is comparable with tankyrase-1 in binding to TRF1. Moreover, tankyrase-2 associates and co-localizes with tankyrase-1 *in vivo*. Our results therefore suggest extensive functional overlap between tankyrase-2 and tankyrase-1.

EXPERIMENTAL

Expression vectors

pIRAP-*myc* and pFLAG-TNKS-1 have been described previously [3]. For pGST-FLAG-HPS (in which GST stands for glutathione S-transferase), the region in pFLAG-TNKS-1 encoding a FLAG (Asp-Tyr-Lys-Asp-Asp-Asp-Asp-Lys)-tagged HPS domain of tankyrase-1 (residues 2–181) was amplified by PCR and inserted into pGEX-4T1 (Amersham Pharmacia) between the *Eco*RI and *Not*I sites. pGST-TRF1 and pGST-IRAP have been described [3] and express GST fused C-terminally to human $TRF1_{1-68}$ and $IRAP_{2-109}$ respectively. pHA-TNKS-1 was derived by replacing the *Spe*I–*Bam*H1 region of pTT20 [1] containing the start codon with a PCR product that contained a Kozac sequence (CCACC) and a haemagglutinin (HA) epitope before the second tankyrase-1 codon. pFLAG-TNKS-2 was derived by inserting two fragments of human TNKS-2 cDNA (GenBank® accession no. AF309033) between the *Not*I and *Sal*I sites of pFLAG-CMV2 (Kodak): a PCR fragment encoding nt 255–985 and digested with *Not*I and *Kpn*I, and a *Kpn*I-*Sal*I fragment encoding nt 986–4725 and obtained from a λgt11 cDNA clone of a skeletal muscle library (ClonTech). For pTNKS-2-FLAG-M1054V, TNKS-2 cDNA was inserted into pcDNA3.1(−)/*Myc*-His.A (Invitrogen) between the *Xba*I and *Bam*H1 sites in three pieces: a PCR fragment digested with *Xba*I and *Xho*I containing a Kozac sequence (CCACC) and TNKS-2 nt 252–606, an *Xho*I–*Bsp*E1 fragment containing TNKS-2 nt 607–3053, and a *Bsp*E1–*Bam*H1 PCR fragment encoding TNKS-2 nt 3054–3749 with an A → G mutation at nt 3411 and a C-terminal FLAG epitope. The verification of the above expression vectors included sequencing of the PCR-derived regions.

Yeast two-hybrid screen

cDNA encoding IRAP residues 2–109 (GenBank® accession no. U62768) was amplified by PCR from a human skeletal muscle two-hybrid library (ClonTech) and inserted between the *Eco*RI and *Bam*H1 sites of pGBDuC(1) [20] to fuse it with the GAL4 DNA-binding domain. This bait construct was transformed into mating type a of the yeast strain PJ69-4, in which interaction with the prey results in both Ade^+ and His^+ phenotypes [20]. The opposite mating type, PJ69-4α, was transformed with a two-hybrid library of human skeletal muscle cDNA (ClonTech). The library was introduced to the IRAP bait by following a mating protocol [21]. Diploids (2×10^8) were plated on ten adenine drop-out plates (15 cm) to select for candidate interactors. The prey plasmids from eight Ade^+ clones recapitulated the Ade^+ phenotype when purified and reintroduced to the bait through mating. They were found by DNA sequencing to encode regions A (residues 153–598; one hit) and B (residues 436–1166; seven hits) of tankyrase-2 (GenBank® accession no. AF 309033) (see Figure 3A). Clone A was also recovered as an interactor when the same library was screened with a smaller IRAP bait (residues 55–109), and the interactors were selected in histidine drop-out plates supplemented with 30 mM 3-aminotriazole (Sigma). To define the regions in tankyrase-2 that interacted with IRAP, clone B was digested completely with *Bam*H1 and partly with *Bgl*II; fragments encoding regions C–E of tankyrase-2 (see Figure 3A) were fused in-frame with the GAL4 activating domain by inserting into the *Bam*H1 site of pGADc(1) [20]. PJ69-4α expressing various tankyrase-2 regions was mated with PJ69-4a expressing the $IRAP_{55-109}$ bait. Diploids were selected in Ura^-Leu^- medium. Saturated cultures (10 μl) were washed in 10% (v/v) glycerol and spotted either on His^- drop-out plates containing 10 mM 3-aminotriazole or on Ura^-Leu^- drop-out plates. To show specificity of the interaction, PJ69-4α expressing tankyrase-2 fragments was similarly mated with a panel of PJ69-4a expressing control baits, such as the C-terminal tail (residues 465–509) of GLUT4, and three irrelevant kinases, TPK-1, TPK-2 and TPK-3 [21].

RNA analysis

Poly(A)$^+$ RNA species (2.5 μg per lane) from 3T3-L1 fibroblasts and day 8 3T3-L1 adipocytes, along with RNA size markers (Gibco), were resolved in a denaturing 1.2% (w/v) agarose gel. The samples were transferred to Nytran Plus (Schleicher & Schuell), immobilized by cross-linking with UV and probed alongside a commercial blot of human mRNA samples [2 μg of poly(A)$^+$ RNA per lane; ClonTech MTN] in ExpressHyb solution (ClonTech) at 65 °C for 1 h in accordance with the manufacturer's recommendation. The probes encoded TNKS-1 (the 3.5 kb *Eco*RI fragment of pTT20 [1]), TNKS-2 (fragment B in Figure 3A) or mouse HSP70, each labelled with [α-^{32}P]dCTP in a ReadyToGo kit (Pharmacia). The blots were washed in 0.1 × SSC/0.1% SDS at 50 °C for 1 h and exposed to BioMax MR films (Kodak).

Transfection and assays

BOSC cells were transfected as described [3] in 6 cm plates with pFLAG-TNKS-1, pFLAG-TNKS-2, pHA-TNKS-1 and pIRAP-*myc*, either individually (5 μg of DNA per plate) or in

pairs (2.5 μg of each vector per plate). The preparation of cell lysates and GST fusions, the washing of immunoprecipitants and affinity-precipitants, the separation of samples by SDS/PAGE and the secondary antibodies used for immunoblotting were as described [3].

For affinity purification, cell lysates from each plate were incubated at 4 °C overnight with resins containing 12 μg of GST, GST–IRAP$_{2-109}$ or GST–TRF1$_{1-68}$ [3].

For co-immunoprecipitation, cell lysates were incubated overnight at 4 °C with FLAG-affinity resins (M2; Sigma) (6 μl), anti-*myc* affinity resins (9E10; Covance) (6 μl) or anti-HA antibody [3 μg of 3F10 (Boehringer Mannheim) for Figure 5; 8 μl of polyclonal HA.11 (Covance) for Figure 9] followed by Protein G–Sepharose (Pharmacia) (8 μl).

For PARP assays in Figure 10(C), lysates were prepared in buffer A [3] from BOSC cells transfected with pFLAG-TNKS-1 or pFLAG-TNKS-2 and precleared by incubation with GST (100 μg per 5.4 mg of lysates) for 1 h. To compensate for the higher expression level of pFLAG-TNKS-2 than that of pFLAG-TNKS-1, lysates expressing pFLAG-TNKS-2 were diluted 1:1 with mock-transfected lysates. Lysates (5.4 mg) were then affinity-precipitated overnight with 30 μg of GST–IRAP$_{78-108}$. After being washed in buffers A (twice) and N (four times) [3], FLAG-tankyrase in the affinity precipitants was quantified on anti-FLAG immunoblots by interpolation between various amounts of GST–FLAG-HPS, which in turn was quantified in Coomassie-stained gels by comparison against an albumin standard (Pierce). To quantify the PARP activity, affinity-precipitated tankyrase was incubated with [*adenylate*-^{32}P]NAD$^+$ (Perkin Elmer) (500 μM at 9.6 Ci/mol, or 21 d.p.m./pmol) in 60 μl of buffer N in a 37 °C rocking water bath for 5 min. The reaction was stopped by the addition of cold buffer A containing 30 mM niacinamide (Sigma). Unincorporated NAD$^+$ was removed by four washes in the same buffer. {In comparison with precipitation with trichloroacetic acid [22], this washing procedure recovered approx. 10 % more radioactivity bound to proteins (results not shown).} Protein-bound radioactivity (in d.p.m.) was divided by the specific activity of [^{32}P]NAD$^+$ to quantify the production of protein-bound ADP-ribose. Background activity due to endogenous ADP-ribosylases was determined in parallel by using mock-transfected lysates. For PARP assays in Figures 10(A) and 10(B), cell lysates were immunoprecipitated with FLAG affinity resins (4 μl per plate) for 2 h at 4 °C. The precipitants were washed in buffer A [3] without niacinamide, equilibrated in buffer N (500 μl) and incubated with 1 mM NAD$^+$ (Sigma) at 37 or 20 °C as indicated.

For immunoblotting, the primary antibodies were anti-poly-(ADP-ribose) (SA-216, 1:1500 dilution; BioMol), anti-FLAG (M2, 1:1000 dilution; Sigma), polyclonal anti-HA.11 (1:1000 dilution; Covance) and anti-*myc* (9E10, 1:1000 dilution; Covance).

Immunofluorescence analysis

COS-7 cells (A.T.C.C.) grown on coverslips in six-well plates were co-transfected with pHA-TNKS-1 (1.8 μg) and pFLAG-TNKS-2 (0.8 μg) by using FuGene 6 (Roche) in accordance with the manufacturer's recommendation. Cells were fixed at 48 h with formaldehyde and processed for immunofluorescence study as described [3]. The primary antibodies were a mouse M2 anti-FLAG antibody (0.8 μg/ml) and a rabbit HA.11 antibody (15 μg/ml). The secondary antibodies were goat anti-mouse (Cy3-conjugated, 1.2 μg/ml; Jackson) and anti-rabbit (FITC-conjugated, 2 μg/ml; Jackson) antibodies. Confocal immunofluorescence images were acquired as described [3].

Metabolic labelling

Adipocytes (3T3-L1) cultured as described [3] were metabolically labelled for 4 h in serum-free Dulbecco's modified Eagle's medium containing 0.1 mCi/ml ^{35}S in EasyTag Express Protein Labeling Mix (Perkin Elmer). The cells were stimulated with or without insulin (1 μg/ml; Sigma) for 15 min and lysed as described [3]. Lysates were precleared by incubation with GST resins (50 μg per 10 cm plate) at 4 °C for 90 min and divided into two aliquots, each incubated with either GST or GST–IRAP$_{96-101}$ (10 μg) at 4 °C for 6 h. The affinity precipitants were resolved by SDS/PAGE [6.5 % (w/v) gel], then dried on paper and exposed to BioMax MR films. The tankyrase-1 band was visible after a 14 h exposure. A 6-day exposure is shown in Figure 8.

RESULTS

Both tankyrase-1 and tankyrase-2 bind to TRF1 and IRAP *in vitro*

Tankyrase-1 and tankyrase-2 reportedly differ in their binding specificity, because only tankyrase-1 interacted with TRF1 in a yeast two-hybrid system [17]. To compare their binding specificity in pull-down assays, lysates of cells expressing recombinant tankyrase-1 or tankyrase-2 were incubated with resins containing either human TRF1$_{1-68}$ or IRAP$_{2-109}$ as GST fusion proteins. Figure 1 shows that both GST–IRAP$_{2-109}$ and GST–TRF1$_{1-68}$ precipitated FLAG-tagged tankyrase-1 and tankyrase-2 comparably (lanes 3–6). The affinity-precipitation was specific, because neither tankyrase was captured by GST alone (Figure 1, lanes 1–2). When tankyrase-2 was ^{35}S-labelled *in vitro* by a coupled transcription/translation system, it was also efficiently affinity-precipitated by GST fusions containing TRF1$_{1-68}$, IRAP$_{2-109}$ or an IRAP hexapeptide (R^{96}QSPDG^{101}) but not by the GST control (results not shown). Therefore tankyrase-2 is indistinguishable from tankyrase-1 in its direct and specific binding to both TRF1 and IRAP.

Tankryase-2 binds to IRAP *in vivo*

In view of the binding between tankyrase-2 and IRAP *in vitro*, their association was also examined *in vivo*. We expressed FLAG-tagged tankyrase-2 and *myc*-tagged IRAP in transfected cells, both individually and simultaneously. The expression of full-length proteins is shown in Figures 2(A) and 2(B). We found that tankyrase-2 co-immunoprecipitated with IRAP (Figure 2C) and, conversely, IRAP co-immunoprecipitated with tankyrase-2 (Figure 2D). The co-immunoprecipitation was specific, because it depended on the simultaneous expression of both proteins (compare lanes 1 and 2 with lane 3). We were not able to co-immunoprecipitate endogenous tankyrase-2 with IRAP. However, because both endogenous proteins are recovered in low-density microsomal fractions [17,23], their interaction as demonstrated with recombinant proteins is physiologically plausible.

Redundant IRAP-binding sites in tankyrase-2

The region within tankyrase-2 that binds to IRAP was examined in a yeast two-hybrid system. By using IRAP as a bait to screen a cDNA library, we identified two tankyrase-2 fragments as IRAP interactors: fragments A (residues 153–599, containing approx. 11 ANK repeats) and B (residues 436–1166, containing approx. 9 ANK repeats) (Figure 3A). The interaction was specific, because neither fragment interacted with the C-terminal tail of GLUT4 (Figure 3B) or three irrelevant kinases, TPK-1, TPK-2 and TPK-3 [21] (results not shown). When deletion derivatives of fragment B were tested in the yeast two-hybrid

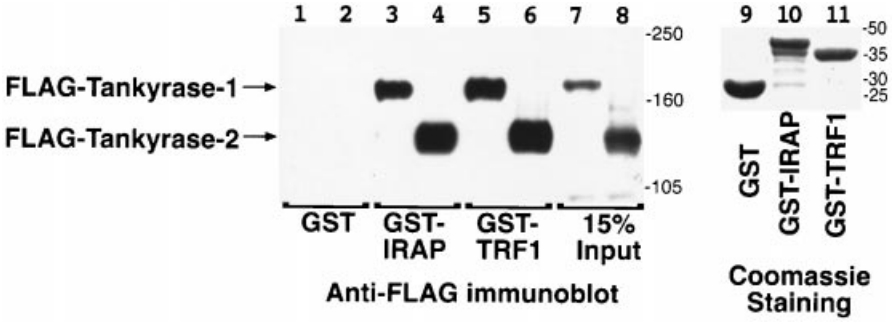

Figure 1 Both tankyrase-1 and tankyrase-2 bind to IRAP and TRF1 *in vitro*

Lysates of cells transiently transfected with either FLAG-tagged tankyrase-1 (lanes 1, 3 and 5) or tankyrase-2 (lanes 2, 4 and 6) were incubated with resins containing GST (lanes 1 and 2), GST fused with human $IRAP_{2–109}$ (lanes 3 and 4) or GST fused with $TRF1_{1–68}$ (lanes 5 and 6) as described in the Experimental section. Resin-bound proteins were resolved by SDS/PAGE alongside 15% of the input lysates (lanes 7 and 8) and immunoblotted with an anti-FLAG antibody as described in the Experimental section. Lanes 9–11 show Coomassie-stained GST, GST–$IRAP_{2–109}$ and GST–$TRF1_{1–68}$ after SDS/PAGE [12% (w/v) gel] (10 μg per lane). The positions of molecular-mass markers are indicated (in kDa) at the right.

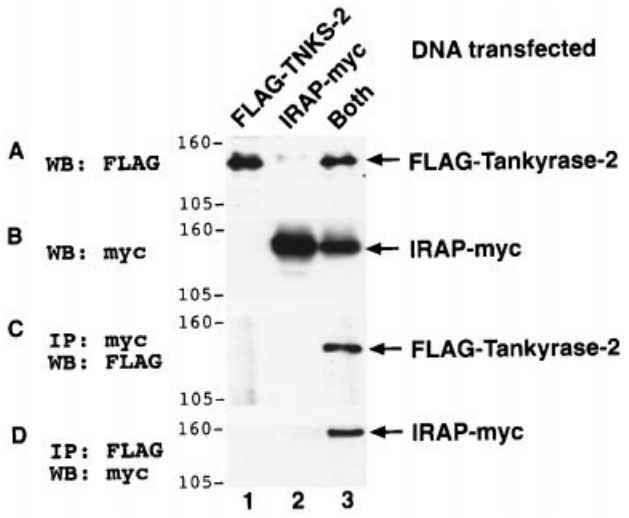

Figure 2 Tankyrase-2 co-immunoprecipitates with IRAP in transfected cells

(**A**, **B**) BOSC cells were transfected with pFLAG-TNKS-2, pIRAP-*myc* or both vectors (lanes 1–3 respectively). Total lysates were immunoblotted (WB) with either an anti-FLAG (**A**) or an anti-*myc* antibody (**B**) as described in the Experimental section. (**C**) Lysates were immunoprecipitated (IP) with an anti-*myc* antibody and immunoblotted with an anti-FLAG antibody. (**D**) Lysastes were immunoprecipitated with an anti-FLAG antibody and immunoblotted with an anti-*myc* antibody.

system, we found that fragments C (residues 436–1088) and D (residues 436–957) also interacted with IRAP, whereas fragment E (residues 436–641) did not (Figure 3B). Because fragment E contained the overlap of fragments A and D, we concluded that the non-overlapping ANK repeats of fragments A and D contributed to IRAP binding. Therefore tankyrase-2 is redundant in that its ANK domain contains (at least) two distinct IRAP-binding sites.

Periodicity among the ANK repeats of tankyrase-2

To help in explaining the observed redundancy in tankyrase-2, we examined the sequence of its ANK repeats, which constitute the interaction domains of many proteins [24]. Within each 33-residue repeat, certain residues are conserved (i.e. the ANK consensus) and specify the folding of the repeat into an L-shaped structure, whereas others are protein-specific and determine the binding specificity of the repeat [25]. Previous analysis has identified 24 ANK repeats in both tankyrase-1 and tankyrase-2 [1,17]. It is noteworthy that nine of these repeats are interrupted by a total of 5 deletions (3–5 residues each) and 7 insertions (5–16 residues each) in a sporadic fashion [1]. This irregular appearance prompted us to propose an alternative analysis that revealed a novel periodicity among the ANK repeats. Our 20-repeat rendition (Figure 3A) depicts the ANK domain of tankyrase-2 (residues 41–798) as comprising 19 full ANK repeats and 2 flanking half-repeats. Moreover, every fourth repeat contains an approx. 22-residue insert; each of the 4 inserts contains an LLEAAR motif or a close variant thereof (Figure 4, right column). This recurrent motif was obscured in previous analysis by being incorporated into various parts of the ANK repeats, namely as residues 1–6, 21–26, 6–11 and 21–26 of repeats 6, 10, 15 and 19 respectively [1]. Because this LLEAAR motif is a poor match for the ANK-repeat consensus, we depicted it as part of an insert to highlight its periodic recurrence, which is conserved by both mammalian and *Drosophila* tankyrases (GenBank® accession no. AF132196, and results not shown).

This four-repeat periodicity also applies to the ANK repeats that are not interrupted by inserts (Figure 4, left column). For instance, repeats 2, 6, 14 and 18 are separated by multiples of four and share the highest pairwise identity of 58–84%. By contrast, repeats 1–3 share a low pairwise identity of 14–46% (results not shown). The same periodicity can also be shown with tankyrase-1 and with the *Drosophila* tankyrase (results not shown). Therefore the ANK domain of tankyrases comprises five similar subdomains; each subdomain contains four ANK repeats and is demarcated by LLEAAR-containing inserts. The similarity between the subdomains indicates structural redundancy within the ANK domain, which is consistent with the redundant binding sites in tankyrase-2 for IRAP (Figure 3B).

Tankyrase-1 and tankyrase-2 associate *in vivo*

Given that the ANK domain of tankyrases can bind to diverse partners (e.g. TRF1, IRAP and Grb14) ([1,3,17], and this study), we examined whether tankyrases could oligomerize into a multivalent scaffold that would bind to multiple partners simultaneously. We therefore expressed HA-tagged tankyrase-1 and FLAG-tagged tankyrase-2, both individually and simul-

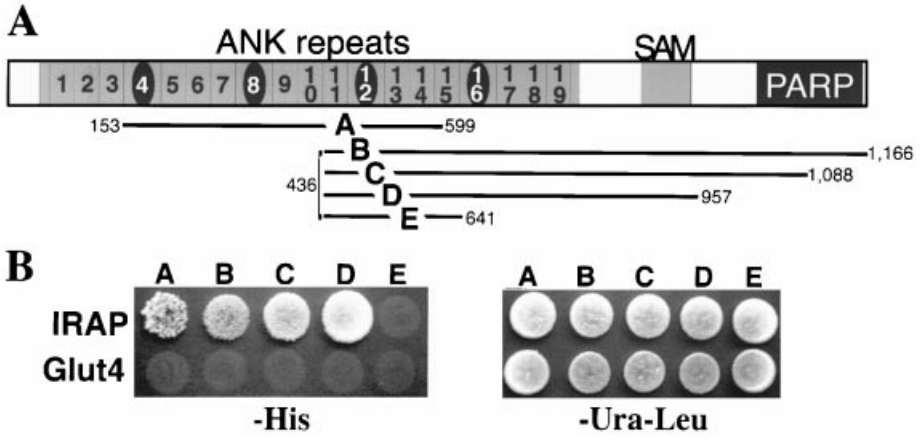

Figure 3 Interaction of tankyrase-2 with IRAP in a two-hybrid system

(**A**) The modular structure of tankyrase-2 is shown in diagrammatic form. Small rectangles represent ANK repeats and follow the numbering shown in Figure 4. Ovals within rectangles represent inserts. (**B**) Fragments A–E of tankyrase-2 as delineated in (**A**) were scored for their interaction with IRAP (upper rows) based on growth on histidine drop-out plates (left panel) in the yeast two-hybrid system as described in the Experimental section, with the use of GLUT4 (lower rows) as a control for specificity. The right panel shows that comparable amounts of yeasts were scored for interaction.

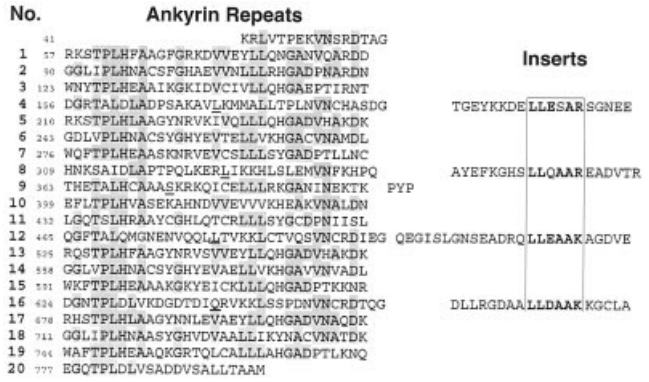

Figure 4 Periodicity in the ANK domain of tankyrase-2

The ANK domain of tankyrase-2 (residues 41–798) is represented as 19 ANK repeats and 2 flanking half-repeats. Shaded residues indicate matches to the ANK-repeat consensus [25]. The sequences at the right show inserts that follow the underlined residues in the corresponding ANK repeats to the left. The LLEAAR motif within the inserts is in bold type.

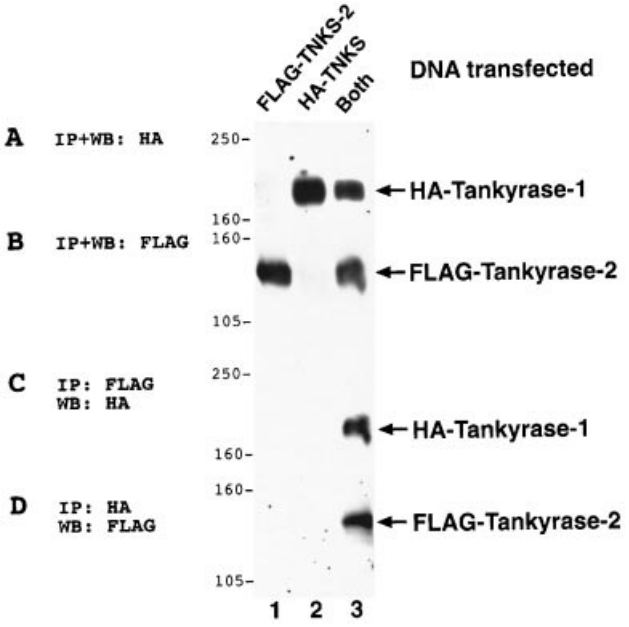

Figure 5 Tankyrase-2 co-immunoprecipitates with tankyrase-1 in transfected cells

BOSC cells were transfected with pFLAG-TNKS-2, pHA-TNKS-1 or both (lanes 1–3 respectively) as described in the Experimental section. Lysates were immunoprecipitated (IP) with anti-FLAG affinity resins and immunoblotted (WB) sequentially with anti-HA (**C**) and then anti-FLAG (**B**) antibodies. Lysates were also immunoprecipitated with an anti-HA antibody and immunoblotted sequentially with anti-FLAG (**D**) and then anti-HA (**A**) antibodies. The positions of molecular-mass markers are indicated (in kDa) at the left.

taneously, in transfected cells (Figure 5). When tankyrase-1 and tankyrase-2 were co-expressed *in vivo*, we recovered tankyrase-1 in tankyrase-2 immunoprecipitants (Figure 5C) and, conversely, tankyrase-2 in tankyrase-1 immunoprecipitants (Figure 5D). As expected, the co-immunoprecipitation did not occur when either protein was expressed alone (lanes 1 and 2). Therefore, recombinant tankyrase-1 and tankyrase-2 can form hetero-oligomers, presumably heterodimers, *in vivo*.

The association of tankyrase-1 with tankyrase-2 also manifests as co-localization in immunofluorescence studies of transfected COS cells. The confocal micrographs in Figure 6 show that both HA–tankyrase-1 (Figure 6A) and FLAG–tankyrase-2 (Figure 6C) displayed a punctate cytosolic pattern with perinuclear accentuation. The merged image in Figure 6(B) shows significant co-localization of tankyrase-1 and tankyrase-2 in vesicular compartments. The observed cytosolic immunostaining clearly exceeded the background staining as defined in mock-transfected cells (results not shown). By contrast, the immunostaining in the nucleus was weak and indistinguishable from the background (results not shown), suggesting that overexpressed tankyrase-1 and tankyrase-2 were predominantly cytoplasmic.

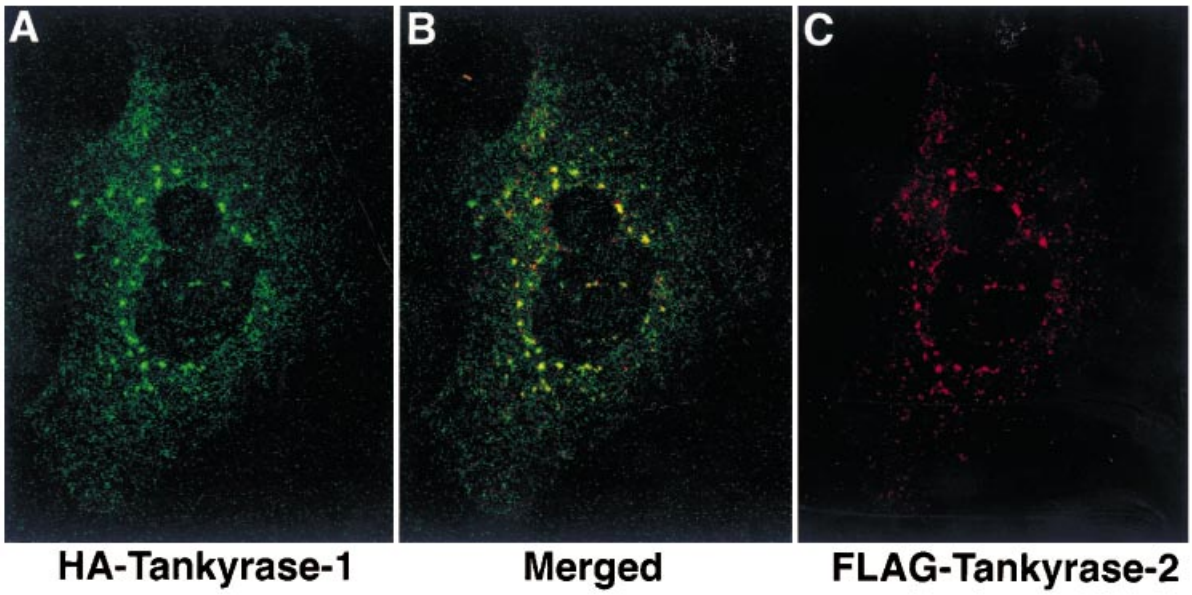

Figure 6 Tankyrase-2 co-localizes with tankyrase-1 in transfected cells

COS cells were co-transfected with pHA-TNKS-1 and pFLAG-TNKS-2, stained for HA and FLAG epitopes and viewed under a confocal microscope as described in the Experimental section. Tankyrase-1 is pseudo-coloured green (**A**) and tankyrase-2 red (**C**). Overlapping red and green pixels are pseudo-coloured yellow in the merged micrograph (**B**).

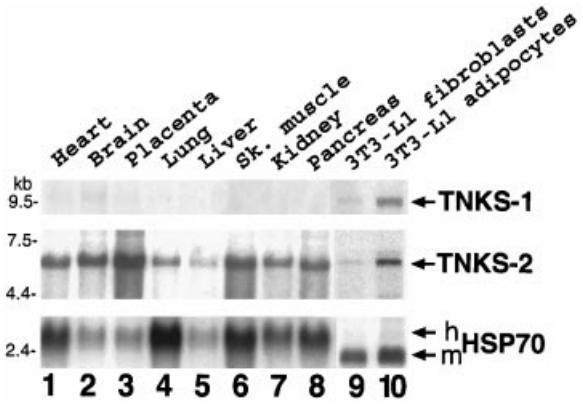

Figure 7 Northern blot analysis of tankyrase-1 and tankyrase-2 mRNA

Poly(A)$^+$ RNA species from eight human tissues (lanes 1–8) and from mouse 3T3-L1 fibroblasts (lane 9) and adipocytes (lane 10) were hybridized with ^{32}P-labelled cDNA probes encoding human tankyrase-1 (top panel), tankyrase-2 (middle panel) or mouse HSP70 (bottom panel) as described in the Experimental section. Transcripts of TNKS-1, TNKS-2, human (h) HSP70 and mouse (m) HSP70 are indicated. Sk. muscle, skeletal muscle.

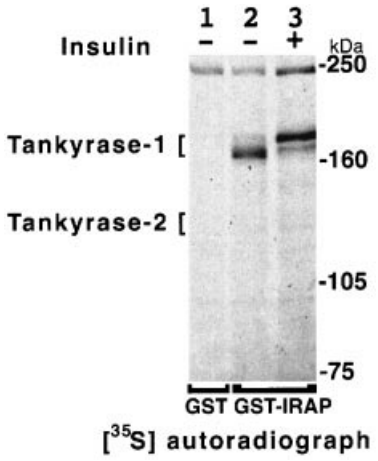

Figure 8 Affinity precipitation of endogenous tankyrase proteins from adipocytes

3T3-L1 adipocytes were metabolically labelled with ^{35}S and stimulated with (lane 3) or without insulin (lanes 1 and 2) as described in the Experimental section. Lysates were incubated with resins containing either GST (lane 1) or GST–IRAP$_{96–101}$ (lanes 2 and 3); the resin-bound proteins were resolved by SDS/PAGE and autoradiographed as described in the Experimental section. The gel mobility of tankyrase-2, which is not detectable by autoradiography, was determined by immunoblotting GST–IRAP affinity-precipitants of non-radiolabelled lysates with the anti-tankyrase antibody T12 [3]. The positions of molecular-mass markers are indicated (in kDa) at the right.

Discordant expression profiles of tankyrase-1 and tankyrase-2

Given that both tankyrases are widely expressed [1,17,19] and can heterodimerize (Figure 5), we compared their expression profiles to determine whether heterodimeric forms might prevail in most tissues. We probed mRNA blots from a panel of sources with ^{32}P-labelled tankyrase-1 and tankyrase-2 cDNA species, with the use of HSP70 cDNA for normalization. Figure 7 shows that tankyrases differed in their expression profiles: tankyrase-1 transcript (approx. 10 kb) was most abundant in adipocytes among the sources examined (lane 10), whereas tankyrase-2 transcript (approx. 6 kb) was most abundant in the placenta (lane 3). The discordant profiles suggest that tankyrase-1 and tankyrase-2 are not exclusively heterodimeric. Despite the different profiles, tankyrase-1 and tankyrase-2 probably share certain regulatory elements, because both genes were induced

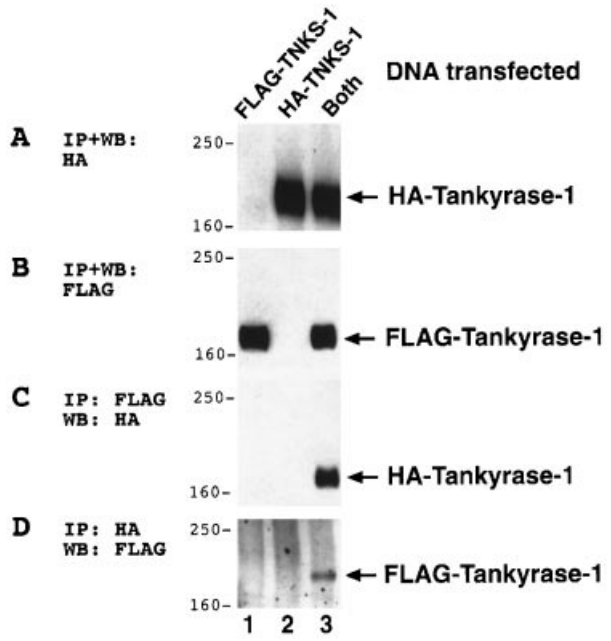

Figure 9 Tankyrase-1 homo-oligomerizes in transfected cells

BOSC cells were transfected with pFLAG-TNKS-1, pHA-TNKS-1 or both (lanes 1–3 respectively) as described in the Experimental section. Lysates were immunoprecipitated (IP) with anti-FLAG affinity resins and immunoblotted (WB) sequentially with anti-HA (**C**) and anti-FLAG (**B**) antibodies. Lysates were also immunoprecipitated with an anti-HA antibody and immunoblotted sequentially with anti-FLAG (**D**) and anti-HA (**A**) antibodies.

approx. 3-fold during the adipogenic differentiation of fibroblasts (Figure 7, compare lanes 9 and 10).

The expression of tankyrase-1 and tankyrase-2 was also compared at the protein level. Taking advantage of the efficient recovery of both tankyrases by GST–IRAP resins (Figure 1), we incubated lysates of adipocytes ^{35}S-labelled *in vivo* with either GST–IRAP$_{96–101}$ or GST resins. Autoradiography of the affinity precipitants revealed a major 165 kDa protein that bound specifically to GST–IRAP (Figure 8, lane 2). This IRAP-binding protein was confirmed as tankyrase-1 on the basis of its 165–175 kDa mobility shift after stimulation by insulin (Figure 8, lanes 2 and 3). This characteristic 10 kDa shift results from the insulin-induced phosphorylation of tankyrase-1 [3]. It is noteworthy that the autoradiograph in Figure 8 did not detect a band between 130 and 140 kDa, where tankyrase-2 was detected when non-radiolabelled adipocyte lysates were immunoblotted (results not shown). Adipocytes therefore express much more tankyrase-1 than tankyrase-2, suggesting that only a fraction of tankyrase-1 in adipocytes exists as hetero-oligomers with tankyrase-2.

In addition to hetero-oligomerization, tankyrases can also homo-oligomerize. In cells expressing both HA-tagged and FLAG-tagged tankyrase-1 (Figure 9), HA–tankyrase-1 was detected in anti-FLAG immunoprecipitants (Figure 9C) and, conversely, FLAG–tankyrase-1 was detected in anti-HA immunoprecipitants (Figure 9D). This co-immunoprecipitation was not observed when tankyrase-1 tagged only with one epitope was expressed (Figure 9, compare lanes 1 and 2 with lane 3). Tankyrases can therefore form both homotypic and heterotypic complexes *in vivo*.

Intrinsic PARP activity of tankyrase-2

Both tankyrases bear C-terminal homology to the catalytic domain of PARP-1 [1,17]. However, the expected PARP activity has been verified only with tankyrase-1 [1]. Tankyrase-2 could therefore be a pseudoenzyme that exerts a dominant-negative effect over tankyrase-1 by, say, competing for shared substrates. We therefore immunoprecipitated FLAG–tankyrase-2 from cell lysates and examined its PARP activity. When supplemented with the PARP cofactor, NAD^+, tankyrase-2 immunoprecipitants formed an extensive smear that stained intensely on anti-poly(ADP-ribose) immunoblots (Figure 10A, left panel,

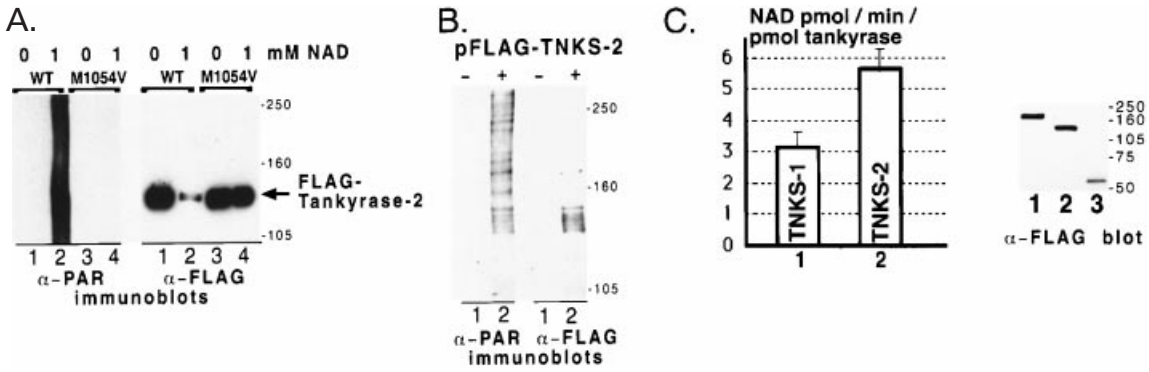

Figure 10 Tankyrase-2 is a PARP

(**A**) FLAG-tagged tankyrase-2, either wild-type (lanes 1 and 2) or with an M1054V substitution (lanes 3 and 4), was immunoprecipitated from transfected cells and incubated for 12 min with (lanes 2 and 4) or without (lanes 1 and 3) 1 mM NAD^+ at 37 °C as described in the Experimental section. Duplicate samples were immunoblotted with either an anti-poly(ADP-ribose) (α-PAR) antibody (left panel) or an anti-FLAG (α-FLAG) antibody (right panel) as described in the Experimental section. (**B**) Lysates from BOSC cells mock-transfected (lane 1) or transfected with pFLAG-TNKS-2 (lane 2) were immunoprecipitated with anti-FLAG antibodies. The immunoprecipitated proteins were incubated for 10 min with 1 mM NAD^+ at 20 °C, resolved by SDS/PAGE and immunoblotted with antibodies against poly(ADP-ribose) (left panel) and the FLAG epitope (right panel). (**C**) FLAG-tagged tankyrase-1 (0.59 pmol, column 1) or tankyrase-2 (0.55 pmol, column 2) was incubated with [^{32}P]NAD^+ at 37 °C for 5 min. The transfer of radiolabel from NAD^+ to protein substrates calculated as described in the Experimental section is expressed as the number of NAD^+ molecules converted per minute per tankyrase molecule into protein-bound ADP-ribose. Results are means $\pm$ S.D. The anti-FLAG immunoblot shows FLAG-tagged tankyrase-1, tankyrase-2 and the protein standard GST–FLAG-HPS (0.22, 0.21 and 0.16 pmol in lanes 1–3 respectively) quantified as described in the Experimental section. The positions of molecular-mass markers are indicated (in kDa) at the right.

lane 2). The intense staining presumably reflected the polymeric nature of the ADP-ribose epitope produced by PARP reactions [26]. Concomitant with the smear formation, tankyrase-2 showed decreased staining on anti-FLAG immunoblots (Figure 10A, right panel, lane 2). This decrease was presumably due to PARP reaction causing heterogeneous retardation of tankyrase-2 in the gel, consequently diluting it to below the detection limit. To confirm this, we curtailed the reaction by lowering the temperature from 37 °C to 20 °C. This did indeed allow the detection of a ladder of tankyrase-2 in both anti-poly(ADP-ribose) and anti-FLAG immunoblots (Figure 10B), confirming that tankyrase-2 was poly(ADP-ribosyl)ated *in vitro*. To exclude the possibility that the observed PARP activity was due to endogenous tankyrase-1 that might have co-precipitated with recombinant tankyrase-2, we introduced an M1054V mutation into the PARP domain of FLAG-tagged tankyrase-2. This mutation corresponds to the M890V mutation that abolishes the enzymic activity of PARP-1 [22] and, as expected, it abolished the PARP activity of tankyrase-2 (Figure 10A, compare lanes 2 and 4). Tankyrase-2 therefore has intrinsic PARP activity that depends critically on the Met^{1054} residue.

To compare the PARP activity of tankyrase-2 with that of tankyrase-1, FLAG-tagged tankyrases were affinity-precipitated from transfected cells by using GST–IRAP resins and were incubated with ^{32}P-labelled NAD^+ at the physiological concentration of 0.5 mM [26]. Radiolabelling of proteins through ADP-ribosylation was measured by scintillation counting. The PARP activity of transfected tankyrase was determined by subtracting the background activity as measured in mock-transfected cells. Figure 10(C) shows that each FLAG–tankyrase-2 molecule transferred approx. 6 NAD^+ molecules per min to protein substrates (column 2). This PARP activity slightly exceeded that of tankyrase-1, at approx. 3 NAD^+ molecules per min (Figure 10C, column 1).

DISCUSSION

This study shows that tankyrase-2 shares many features with tankyrase-1. Tankyrase-2 associates with tankyrase-1 *in vivo* and exhibits intrinsic PARP activity *in vitro*. Like tankyrase-1, tankyrase-2 binds to both IRAP and TRF1. Moreover, we have revealed a novel sequence periodicity in the ANK domain of both tankyrase-1 and tankyrase-2 and propose that their ANK domain comprises five subdomains.

The ANK domain of tankyrases is comparable in size (82 kDa) with that of the cytoskeletal protein ankyrin (84 kDa) [27], both of which are significantly larger than the typical ANK domains (14–32 kDa) found in many other proteins [24]. The ANK domain of ankyrin binds to various membrane proteins [28] and comprises four subdomains, each consisting of six ANK repeats [27]. Similarly, the ANK domains of tankyrases bind to diverse partners (such as Grb14, IRAP and TRF1) [1,3,17]. However, no subdomain organization was revealed by a previous analysis of the ANK domain of tankyrases, which was thought to contain multiple irregular insertions and deletions [1].

We present an alternative sequence alignment for the ANK domain of tankyrases that offers several advantages over the previous analysis. Our rendition minimizes the somewhat arbitrary assignment of insertions and deletions to many ANK repeats. Moreover, it reveals a four-repeat periodicity among the ANK repeats of tankyrases and identifies a novel LLEAAR motif that also recurs at a four-repeat interval. We consider this LLEAAR motif as an insertional sequence that is located 22–23 residues upstream of the subsequent ANK repeat (Figure 4). It is noteworthy that the transcription factor GA-binding protein β (GABPβ) [29] also contains an LLEAAR motif (residues 10–15 in GenBank® accession no. Q00420) located 21 residues upstream of its four ANK repeats. Our sequence analysis therefore suggests that a group of four ANK repeats might have annexed the LLEAAR sequence before evolving into both GABPβ and, presumably through quintuplication, the ANK domain of tankyrases. Thus the ANK domain of tankyrases apparently comprises five subdomains; each subdomain consists of four ANK repeats and is demarcated from its adjacent subdomain by an LLEAAR-containing insert.

Two lines of evidence suggest that tankyrases are multivalent in their interaction with partners. First, an individual tankyrase molecule contains five similar subdomains in the ANK domain and provides redundant binding sites as defined by IRAP binding (Figure 3). Secondly, multiple tankyrase molecules can link their ANK domains through oligomerization. How tankyrase-1 and tankyrase-2 oligomerize remains unclear, except that both proteins contain a SAM motif that has been implicated in dimerizing other proteins [30]. The SAM domain of Scm (residues 797–877), for instance, has been shown as a GST fusion to bind *in vitro* to the SAM domain of a protein called ph [31]. Unfortunately, GST fusions containing the SAM domain of either tankyrase-1 (residues 1021–1089) or tankyrase-2 (residues 868–936) failed to bind to full-length tankyrases *in vitro* (results not shown). It therefore remains to be shown that the SAM domain of tankyrases is involved in their oligomerization.

The physiological function of tankyrase-2 has yet to be established. Given that tankyrase-2 associates with tankyrase-1 and that both homologues share similar enzymic and binding activities, tankyrase-2 probably regulates the same cellular processes as have been proposed for tankyrase-1, namely vesicular targeting and telomere homoeostasis [3,6]. More specifically, IRAP binding might allow tankyrase-2 to use its PARP activity to regulate the targeting machinery for IRAP-containing vesicles. A precedent for ADP-ribosylation to regulate vesicular targeting involves the G-protein brefeldin ADP-ribosylation substrate ('BARS'), whose activity in promoting vesicular budding from the Golgi is inhibited by ADP-ribosylation [32,33]. Moreover, the binding of tankyrase-2 to both IRAP and Grb14 might enable IRAP-containing vesicles to interact with signalling molecules that use Grb14 as an adapter. We therefore suspect that tankyrase-2, either by itself or as a complex with tankyrase-1, has a regulatory function in the targeting of IRAP-containing vesicles.

Overexpressed tankyrase-2, like tankyrase-1, is predominantly cytoplasmic (Figure 6), which is consistent with the lack of an NLS in either tankyrase [4]. However, a fraction of endogenous tankyrase-2 might be recruited to telomeres through the binding of TRF1, as has been shown with tankyrase-1 [4]. This would allow the PARP activity of tankyrase-2 to poly(ADP-ribosyl)ate TRF1 and attenuate its affinity for telomeric DNA, in much the same way as tankyrase-1 affects TRF1 [1]. We therefore suspect that tankyrase-2 shares the antagonistic effect of tankyrase-1 on TRF1 at telomeres. The predominant targeting of both tankyrases to the cytosol is reminiscent of that of PARG, a glycohydrolase that removes poly(ADP-ribose) from PARP substrates. PARG is predominantly cytoplasmic, but a small fraction has been suspected to translocate to the nucleus [34].

The remarkable functional similarity shown here between tankyrase-1 and tankyrase-2 is in keeping with their extensive sequence similarity. Conversely, their sequence divergence, albeit limited, might endow each tankyrase with distinct properties. The greatest sequence divergence is in the HPS domain, which is unique to tankyrase-1 [17]. This 180-residue region shows little similarity to other proteins [1], but it harbours all four of the

MAP kinase consensus sites (PXSP) [35] of tankyrase-1 [17]. The second highest divergence is at the junction of the ANK domain and the SAM motif (residues 813–869 in tankyrase-2), where all gaps in the co-linear alignment between tankyrase-1 and tankyrase-2 are found [17]. Curiously, this region harbours the sole MAP kinase consensus site of tankyrase-2 (namely PSSP at residues 829–832). Therefore MAP kinases or other proline-directed protein kinases might conceivably target non-conserved sites in tankyrase-1 and tankyrase-2 and thereby differentially affect their activities. We have shown that MAP kinases serine-phosphorylate tankyrase-1 *in vivo* and that this phosphorylation enhances its PARP activity *in vitro* [3]. The candidate phosphorylation sites in tankyrase-1 have been suspected to be among the MAP kinase consensus sites in the HPS domain [17]. We are investigating whether MAP kinases phosphorylate tankyrase-2 and regulate any of its activity. If the two tankyrases differ in their regulation by upstream kinases, their relative abundances in a given cell might dictate how signalling cascades engage cellular pools of tankyrase-1 and tankyrase-2, which otherwise seem to have indistinguishable activities.

We thank Dr William Schiemann for comments on the manuscript, Dr Titia de Lange for pTT20, Dr G. Todd Milne, Dr Laura Robertson and Dr Phil James for reagents and advice on two-hybrid screens, Dr Ralph Lin for poly(A)$^+$ mRNA from 3T3-L1 cells, Nicki Watson at the W.M. Keck Foundation Imaging Facility for assistance with confocal microscopy, and Dr Jerry Morris for the HSP70 cDNA. This work was supported by NIH grants DK47618 to H.F.L. and DK02540 to N.-W.C.

REFERENCES

1 Smith, S., Giriat, I., Schmitt, A. and de Lange, T. (1998) Tankyrase, a poly(ADP-ribose) polymerase at human telomeres. Science **282**, 1484–1487
2 Ponting, C. P. (1995) SAM: a novel motif in yeast sterile and *Drosophila* polyhomeotic proteins. Protein Sci. **4**, 1928–1930
3 Chi, N.-W. and Lodish, H. F. (2000) Tankyrase is a Golgi-associated mitogen-activated protein kinase substrate that interacts with IRAP in GLUT4 vesicles. J. Biol. Chem. **275**, 38437–38444
4 Smith, S. and de Lange, T. (1999) Cell cycle dependent localization of the telomeric PARP, tankyrase, to nuclear pore complexes and centrosomes. J. Cell Sci. **112**, 3649–3656
5 van Steensel, B. and de Lange, T. (1997) Control of telomere length by the human telomeric protein TRF1. Nature (London) **385**, 740–743
6 Smith, S. and de Lange, T. (2000) Tankyrase promotes telomere elongation in human cells. Curr. Biol. **10**, 1299–1302
7 Mack, G. J., Ou, Y. and Rattner, J. B. (2000) Integrating centrosome structure with protein composition and function in animal cells. Microsc. Res. Tech. **49**, 409–419
8 Pessin, J. E., Thurmond, D. C., Elmendorf, J. S., Coker, K. J. and Okada, S. (1999) Molecular basis of insulin-stimulated GLUT4 vesicle trafficking. Location! Location! Location! J. Biol. Chem. **274**, 2593–2596
9 Kandror, K. V., Yu, L. and Pilch, P. F. (1994) The major protein of GLUT4-containing vesicles, gp160, has aminopeptidase activity. J. Biol. Chem. **269**, 30777–30780
10 Keller, S. R., Scott, H. M., Mastick, C. C., Aebersold, R. and Lienhard, G. E. (1995) Cloning and characterization of a novel insulin-regulated membrane aminopeptidase from Glut4 vesicles. J. Biol. Chem. **270**, 23612–23618
11 Herbst, J. J., Ross, S. A., Scott, H. M., Bobin, S. A., Morris, N. J., Lienhard, G. E. and Keller, S. R. (1997) Insulin stimulates cell surface aminopeptidase activity toward vasopressin in adipocytes. Am. J. Physiol. **272**, E600–E606
12 Czech, M. P. and Corvera, S. (1999) Signaling mechanisms that regulate glucose transport. J. Biol. Chem. **274**, 1865–1868
13 Kozma, L., Baltensperger, K., Klarlund, J., Porras, A., Santos, E. and Czech, M. P. (1993) The ras signaling pathway mimics insulin action on glucose transporter translocation. Proc. Natl. Acad. Sci. U.S.A. **90**, 4460–4464

Received 30 July 2001/31 October 2001; accepted 15 November 2001

14 Yamamoto, Y., Yoshimasa, Y., Koh, M., Suga, J., Masuzaki, H., Ogawa, Y., Hosoda, K., Nishimura, H., Watanabe, Y., Inoue, G. and Nakao, K. (2000) Constitutively active mitogen-activated protein kinase kinase increases GLUT1 expression and recruits both GLUT1 and GLUT4 at the cell surface in 3T3-L1 adipocytes. Diabetes **49**, 332–339
15 Hausdorff, S. F., Frangioni, J. V. and Birnbaum, M. J. (1994) Role of p21ras in insulin-stimulated glucose transport in 3T3-L1 adipocytes. J. Biol. Chem. **269**, 21391–21394
16 Fingar, D. C. and Birnbaum, M. J. (1994) A role for Raf-1 in the divergent signaling pathways mediating insulin- stimulated glucose transport. J. Biol. Chem. **269**, 10127–10132
17 Lyons, R. J., Deane, R., Lynch, D. K., Ye, Z. S., Sanderson, G. M., Eyre, H. J., Sutherland, G. R. and Daly, R. J. (2001) Identification of a novel human tankyrase through its interaction with the adaptor protein Grb14. J. Biol. Chem. **276**, 17172–17180
18 Monz, D., Munnia, A., Comtesse, N., Fischer, U., Steudel, W. I., Feiden, W., Glass, B. and Meese, E. U. (2001) Novel tankyrase-related gene detected with meningioma-specific sera. Clin. Cancer Res. **7**, 113–119
19 Kuimov, A. N., Kuprash, D. V., Petrov, V. N., Vdovichenko, K. K., Scanlan, M. J., Jongeneel, C. V., Lagarkova, M. A. and Nedospasov, S. A. (2001) Cloning and characterization of TNKL, a member of tankyrase gene family. Genes Immun. **2**, 52–55
20 James, P., Halladay, J. and Craig, E. A. (1996) Genomic libraries and a host strain designed for highly efficient two-hybrid selection in yeast. Genetics (Princeton) **144**, 1425–1436
21 Robertson, L. S. and Fink, G. R. (1998) The three yeast A kinases have specific signaling functions in pseudohyphal growth. Proc. Natl. Acad. Sci. U.S.A. **95**, 13783–13787
22 Rolli, V., O'Farrell, M., Menissier-de Murcia, J. and de Murcia, G. (1997) Random mutagenesis of the poly(ADP-ribose) polymerase catalytic domain reveals amino acids involved in polymer branching. Biochemistry **36**, 12147–12154
23 Ross, S. A., Scott, H. M., Morris, N. J., Leung, W. Y., Mao, F., Lienhard, G. E. and Keller, S. R. (1996) Characterization of the insulin-regulated membrane aminopeptidase in 3T3-L1 adipocytes. J. Biol. Chem. **271**, 3328–3332
24 Bork, P. (1993) Hundreds of ankyrin-like repeats in functionally diverse proteins: mobile modules that cross phyla horizontally? Proteins **17**, 363–374
25 Sedgwick, S. G. and Smerdon, S. J. (1999) The ankyrin repeat: a diversity of interactions on a common structural framework. Trends Biochem. Sci. **24**, 311–316
26 D'Amours, D., Desnoyers, S., D'Silva, I. and Poirier, G. G. (1999) Poly(ADP-ribosyl)ation reactions in the regulation of nuclear functions. Biochem. J. **342**, 249–268
27 Michaely, P. and Bennett, V. (1993) The membrane-binding domain of ankyrin contains four independently folded subdomains, each comprised of six ankyrin repeats. J. Biol. Chem. **268**, 22703–22709
28 Michaely, P. and Bennett, V. (1995) Mechanism for binding site diversity on ankyrin. Comparison of binding sites on ankyrin for neurofascin and the Cl^-/HCO_3^- anion exchanger. J. Biol. Chem. **270**, 31298–31302
29 LaMarco, K., Thompson, C. C., Byers, B. P., Walton, E. M. and McKnight, S. L. (1991) Identification of Ets- and notch-related subunits in GA binding protein. Science **253**, 789–792
30 Schultz, J., Ponting, C. P., Hofmann, K. and Bork, P. (1997) SAM as a protein interaction domain involved in developmental regulation. Protein Sci. **6**, 249–253
31 Peterson, A. J., Kyba, M., Bornemann, D., Morgan, K., Brock, H. W. and Simon, J. (1997) A domain shared by the Polycomb group proteins Scm and ph mediates heterotypic and homotypic interactions. Mol. Cell Biol. **17**, 6683–6692
32 Spano, S., Silletta, M. G., Colanzi, A., Alberti, S., Fiucci, G., Valente, C., Fusella, A., Salmona, M., Mironov, A., Luini, A. et al. (1999) Molecular cloning and functional characterization of brefeldin A-ADP-ribosylated substrate. A novel protein involved in the maintenance of the Golgi structure. J. Biol. Chem. **274**, 17705–17710
33 Weigert, R., Silletta, M. G., Spano, S., Turacchio, G., Cericola, C., Colanzi, A., Senatore, S., Mancini, R., Polishchuk, E. V., Salmona, M. et al. (1999) CtBP/BARS induces fission of Golgi membranes by acylating lysophosphatidic acid. Nature (London) **402**, 429–433
34 Affar, E. B., Germain, M., Winstall, E., Vodenicharov, M., Shah, R. G., Salvesen, G. S. and Poirier, G. G. (2001) Caspase-3-mediated processing of poly(ADP-ribose) glycohydrolase during apoptosis. J. Biol Chem. **276**, 2935–2942
35 Davis, R. J. (1993) The mitogen-activated protein kinase signal transduction pathway. J. Biol. Chem. **268**, 14553–14556